JOC Article

Solvation in Electrospray Mass Spectrometry: Effects on the Reaction Kinetics of Fragmentation Mediated by Ion-Neutral Complexes

Ya-Ping Tu,* Limin He, William Fitch, and Michelle Lam

Department of Drug Metabolism and Pharmacokinetics, Roche Pharmaceuticals, 3431 Hillview Ave., Palo Alto, California 94304

yaping.tu@roche.com

Received March 2, 2005

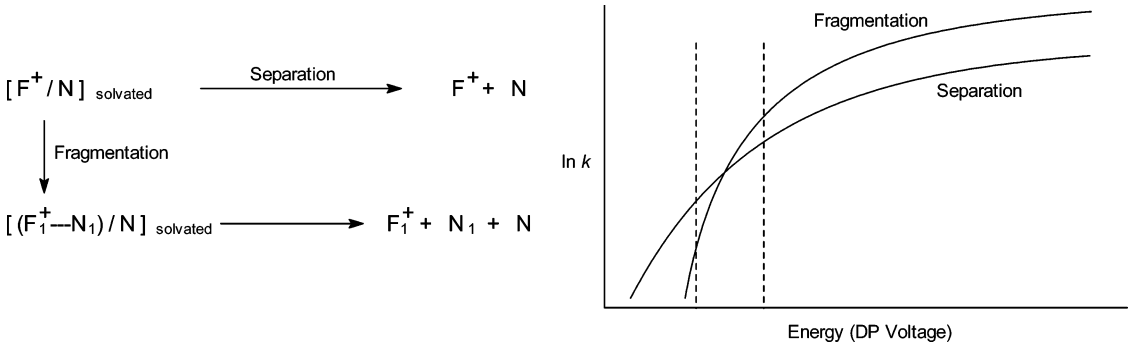

In electrospray ionization (ESI) on a triple quadrupole mass spectrometer, benzydamine, a molecule with an *N*,*N*-dimethylaminopropoxyl side chain, showed a fragmentation pattern in Q1 scans that is dramatically different from the mass-selected collision-induced dissociation (CID) of its MH^+ ion. The *N*,*N*-dimethylimmonium ion, which dominates in Q1 scans at higher energies, is only a minor product in all CID spectra. By using a smaller model molecule, *N*,*N*,*N*′,*N*′-tetramethyl-1,3-propanediamine, with the kinetic energy release measured for the corresponding reaction, we have demonstrated that an ion-neutral complex composed of the *N*,*N*-dimethylazetidine cation and a neutral counterpart is involved. When the ion-neutral complex intermediate evolves toward elimination to form the immonium ion, the transition state is stabilized by the neutral species. Solvation of the ion-neutral complex, which obstructs the separation of the two partners by the resulting tighter enclosure, facilitates the elimination by enhancing the stabilization of the transition state. Therefore, the prevalence of the immonium ion in Q1 scans was a result of solvation in the ESI source. In CID reactions, where the decomposing ions are mass-selected and thus solvation does not exist, the immonium ion was a minor product, and the separation of the ion-neutral complex became dominant.

Introduction

Electrospray ionization mass spectrometry (ESI-MS) is a versatile technique for the analysis of a large variety of molecules and offers a seamless interface with liquid chromatography[1,2] to serve as a tool that is now routinely employed in many areas, such as in the realm of drug discovery, for quantification and structural determination.[3−6] In ESI-MS, the analyte ions in a stream of tiny charged droplets are transferred from atmospheric pressure to vacuum typically through an orifice and further extracted into an ion optics prior to the mass analyzer by means of a skimmer.[7] Also brought into vacuum along with the ions is a large amount of solvent molecules.

(1) (a) Abian, J. *J. Mass Spectrom.* **1999**, *34*, 157−168. (b) Abian, J.; Oosterkamp, A. J.; Gelpi, E. *J. Mass Spectrom.* **1999**, *34*, 244−254.
(2) Tomer, K. B. *Chem. Rev*. **2001**, *101*, 297−328.
(3) Smyth, W. F. *Anal. Chim. Acta* **2003**, *492*, 1−16.
(4) Kostiainen, R.; Kotiao, T.; Kuuranne, T.; Auriola, S. *J. Mass Spectrom*. **2003**, *38*, 357−372.
(5) Atcheson, B.; Taylor, P. J.; Pillans, P. I.; Tett, S. E. *Anal. Chim. Acta* **2003**, *492*, 157−169.
(6) Hopfgartner, G.; Bourgogne, E. *Mass Spectrom. Rev*. **2003**, *22*, 195−214.
(7) (a) Bruins, A. P. In *Electrospray Ionization Mass Spectrometry: Fundamentals, Instrumentation and Applications*; Cole, R. B., Ed.; Wiley: New York, 1997; Chapter 3. (b) Bruins, A. P. *J. Chromatogr. A* **1998**, *794*, 345−357. (c) Niessen, W. M. A. *J. Chromatogr. A* **1998**, *794*, 407−435.

10.1021/jo050398n CCC: $30.25
Published on Web 05/25/2005

Therefore, ions in the orifice-skimmer region are heavily solvated. Collisions between the bulky ions and the background gas molecules result in desolvation to produce ultimately the unsolvated ions, following either the charged residue mechanism or the ion evaporation theory.[8−10] The energy accumulated in collisions can cause not only the solvated ions to strip off the solvent molecules but also the core ions to dissociate. As a result of the combined effects, the mass spectrum shows the molecular ions along with some fragment ions.

Fragmentation reactions occurring in the orifice-skimmer region have been an interesting subject of many studies,[11−14] especially when compared with the mass-selected collision-induced dissociation (CID) in the collision cell of a tandem mass spectrometer. In an ESI source, which serves as an atmosphere/vacuum interface (the free jet expansion occurs here), energy deposition[15] to the ions is much more complicated than in the collision cell.[7,16] However, theoretical modeling and experimental studies[16,17] have shown that the internal energy of the ions gained from collisions with the background gas molecules is linearly correlated with the declustering voltage applied to this region. Therefore, the extent to which fragmentation occurs increases with increasing voltage. This is consistent with the results of other studies where fragmentations in the ion source are compared with those in the collision cell, and it is concluded by Harrison and others[12,13] that reactions at the two venues take place in an essentially *similar* pattern. Unless the stereochemistry is involved in electrospray,[18] as seen in chemical ionization,[19] this conclusion should hold, provided that the energy is the *sole* factor that governs the fragmentation reactions, because the same amount of internal energy can be attained at both sites by adjusting appropriate voltages. However, since ions are highly solvated in electrospray, fragmentation in the ion source may have a strong solvation effect that does not exist at all on reactions in the collision cell where the ions of interest, which are mass-selected, are desolvated completely.

Studies on solvated ions, which are viewed as a bridging system between the gas phase and solution, have provided insights into the role of solvent in the reactions of the ions.[20−26] In *bimolecular* reactions, such as the S_N2 nucleophilic displacement reactions, Brauman et al.[21] have demonstrated that the stabilization energies stemming from solvation are different in the reactant ion and the transition state. A simple ion usually has a large binding energy with a solvent molecule; the transition state, however, has the charge delocalized over a larger area and thus can only be weakly solvated. As a result of this differential solvation, the central energy barrier to the reaction is actually increased compared to that of the unsolvated system.[21] Therefore, the reaction rate constant decreases rapidly with increasing degree of solvation of the reactant ion.[20] On the other hand, when a *unimolecular* reaction of the ions occurs, solvation shows totally different effects. Isomerization of an ion that involves a 1,2-proton transfer, for example, can be catalyzed by a solvent molecule.[23] Direct intraionic proton transfer (in the bare ion), such as that in $CH_3OH^{+\bullet} \rightarrow {}^{\bullet}CH_2OH_2^{+}$, has a high energy barrier. When the ion is solvated, the "solvent" molecule that is attached to the ion can transport, as a carrier, the proton from one site to another.[23−26]

Ion-molecule reactions and the catalyzed isomerizations mentioned above are two specific subjects of studies in the gas phase by mass spectrometry. More routinely seen in mass spectrometry, however, is simply the fragmentation of ions. In the past 2 decades, fragmentation reactions proceeding via an ion-neutral complex intermediate have been well documented.[27−32] When a covalent bond is ruptured, the two incipient fragments can still be held together electrostatically. Before they are separated, some secondary reactions of the ionic partner may take place while the neutral species is still

(8) Dole, M.; Mack, L. L.; Hines, R. L. *J. Chem. Phys*. **1968**, *49*, 2240−2249.
(9) (a) Iribarne, J. V.; Thomson, B. A. *J. Chem. Phys*. **1976**, *64*, 2287−2294. (b) Thomson, B. A.; Iribarne, J. V. *J. Chem. Phys*. **1979**, *71*, 4451−4463.
(10) Kebarle, P. *J. Mass Spectrom*. **2000**, *35*, 804−817.
(11) (a) Thomson, B. A. *J. Am. Soc. Mass Spectrom*. **1997**, *8*, 1053−1058. (b) Serani, L.; Lemaire, D.; Laprevote, O. *Int. J. Mass Spectrom*. **2002**, *219*, 403−408.
(12) (a) Harrison, A. G. *Rapid Commun. Mass Spectrom*. **1999**, *13*, 1663−1670. (b) Harrison, A. G. *J. Mass Spectrom*. **1999**, *34*, 1253−1273. (c) van Dongen, W. D.; van Wijk, J. I. T.; Green, B. N.; Heerma, W.; Haverkamp, J. *Rapid Commun. Mass Spectrom*. **1999**, *13*, 1712−1716.
(13) Bure, C.; Lange, C. *Curr. Org. Chem*. **2003**, *7*, 1613−1624.
(14) (a) Weinmann, W.; Wiedemann, A.; Eppinger, B.; Renz, M.; Svoboda, M. *J. Am. Soc. Mass Spectrom*. **1999**, *10*, 1028−1037. (b) Weinmann, W.; Stoertzel, M.; Vogt, S.; Wendt, J. *J. Chromatogr. A* **2001**, *926*, 199−209. (c) Weinmann, W.; Stoertzel, M.; Vogt, S.; Svoboda, M.; Schreiber, A. *J. Mass Spectrom*. **2001**, *36*, 1013−1023. (d) Bure, C.; Gobert, W.; Lelievre, D.; Delmas, A. *J. Mass Spectrom*. **2001**, *36*, 1149−1155. (e) Bristow, A. W. T.; Nichols, W. F.; Webb, K. S.; Conway, B. *Rapid Commun. Mass Spectrom*. **2002**, *16*, 2374−2386.
(15) Gabelica, V.; De Pauw, E. *Mass Spectrom. Rev*. In press.
(16) (a) Schneider, B. B.; Chen, D. D. Y. *Anal. Chem*. **2000**, *72*, 791−799. (b). Schneider, B. B.; Douglas, D. J.; Chen, D. D. Y. *Rapid Commun. Mass Spectrom*. **2001**, *15*, 249−257.
(17) (a) Collette, C.; De Pauw, E. *Rapid Commun. Mass Spectrom*. **1998**, *12*, 165−170. (b) Collette, C.; Drahos, L.; De Pauw, E.; Vekey, K. *Rapid Commun. Mass Spectrom*. **1998**, *12*, 1673−1678. (c) Gabelica, V.; De Pauw, E.; Karas, M. *Int. J. Mass Spectrom*. **2004**, *231*, 189−195. (d). Naban-Maillet, J.; Lesage, D.; Bossee, A.; Gimbert, Y.; Sztaray, J.; Vekey, K.; Tabet, J. C. *J. Mass Spectrom*. **2005**, *40*, 1−8.
(18) Laprevote, O.; Ducrot, P.; Thal, C.; Serani, L.; Das, B. C. *J. Mass Spectrom*. **1996**, *31*, 1149−1155.
(19) (a) Weisz, A.; Cojocaru, M.; Mandelbaum, A. *J. Chem. Soc., Chem. Commun*. **1989**, 331−332. (b) Morlender-Vais, N.; Mandelbaum, A. *J. Mass Spectrom*. **1999**, *34*, 291−302. (c) Vais, V.; Etinger, A.; Mandelbaum, A. *J. Mass Spectrom*. **1999**, *34*, 755−760. (d) Denekamp, C.; Mandelbaum, A. *J. Mass Spectrom*. **2001**, *36*, 422−429.
(20) (a) Bohme, D. K.; Mackay, G. I. *J. Am. Chem. Soc*. **1981**, *103*, 979−981. (b) Bohme, D. K.; Raksit, A. B.; Mackay, G. I. *J. Am. Chem. Soc*. **1982**, *104*, 1100−1101. (c) Bohme, D. K.; Raksit, A. B. *J. Am. Chem. Soc*. **1984**, *106*, 3447−3452.
(21) (a) Chabinyc, M. L.; Craig, S. L.; Regan, C. K.; Brauman, J. I. *Science* **1998**, *279*, 1882−1886. (b) Craig, S.; Brauman, J. I. *J. Am. Chem. Soc*. **1999**, *121*, 6690−6699. (c) Regan, C. K.; Craig, S. L.; Brauman, J. I. *Science* **2002**, *295*, 2245−2247.
(22) Takashima, K.; Riveros, J. M. *Mass Spectrom. Rev*. **1998**, *17*, 409−430.
(23) Bohme, D. K. *Int. J. Mass Spectrom* **1992**, *115*, 95−110.
(24) (a) Gauld, J. W.; Audier, H.; Fossey. J.; Radom, L. *J. Am. Chem. Soc*. **1996**, *118*, 6299−6300. (b) Gauld, J. W.; Radom, L. *J. Am. Chem. Soc*. **1997**,*119*, 9831−9839.
(25) Trikoupis, M. A.; Terlouw, J. K.; Burgers, P. C. *J. Am. Chem. Soc*. **1998**, *120*, 12131−12132.
(26) Tu, Y.-P.; Holmes, J. L. *J. Am. Chem. Soc*. **2000**, *122*, 3695−3700; 5597−5602.
(27) Williams, D. H. *Acc. Chem. Res*. **1977**, *10*, 280−286.
(28) (a) Morton, T. H. *Tetrahedron* **1982**, *38*, 3195−3243. (b) Morton, T. H. *Org. Mass Spectrom*. **1992**, *27*, 353−368.
(29) (a) McAdoo, D. J. *Mass Spectrom. Rev*. **1988**, *7*, 363−393. (b) McAdoo D. J.; Morton, T. H. *Acc. Chem. Res*. **1993**, *26*, 295−302.
(30) Bowen, R. D. *Acc. Chem. Res*. **1991**, *24*, 364−371.
(31) Longevialle, P. *Mass Spectrom. Rev*. **1992**, *11*, 157−192.
(32) Chalk, A. J.; Radom, L. *J. Am. Chem. Soc*. **1998**, *120*, 8430−8437.

attached to it, as if both were trapped in a cage. This is why the intermediacy of ion-neutral complexes is also reviewed as the gas-phase analogue of the cage effect,[29b] which is a typical solvent influence on reactions in solution. Given the fact that electrospray is now a dominant ionization technique and ions are heavily solvated in the source region, as stated earlier, a simple question arises. Does or how does solvation affect a fragmentation reaction that involves an intermediate ion-neutral complex in electrospray? In particular, we would like to see if solvation would enhance the "cage effect" to favor secondary *fragmentation* over the simple *separation* of the complex. In this paper we describe the mass spectrometry of benzydamine, a drug molecule, which showed a drastic difference in fragmentation between the orifice-skimmer region and the collision cell. Solvation in the ion source enhanced an ion-neutral complex leading to a secondary fragmentation that was hardly seen in the mass-selected CID of the molecular ions in the collision cell.

Experimental Section

Unless indicated otherwise, ESI data discussed here were obtained by using a Sciex API 300 triple quadrupole mass spectrometer (MDS Sciex, Toronto, Ontario, Canada) with a turbo ionspray source and the Analyst software package. The source was operated at a temperature of 120 °C and an electrospray voltage at 4500 V. Zero air was used as the desolvating gas and nitrogen as the curtain gas. The collision gas was also nitrogen at a pressure of 2.5×10^{-5} Torr (1 Torr = 133.3 Pa) as read in the ion gauge that is attached to the collision cell. A Sciex API 4000 with an orthogonal turbo V spray source and a Waters/Micromass Ultima with a Z-spray source (both are triple quadrupoles) were also used for comparison. Accurate mass data were obtained on a Micromass API-US hybrid quadrupole/time-of-flight (Q-TOF) mass spectrometer with a lockspray for the reference material at a resolution of ~10,000. The collision gas was argon on both Micromass instruments. A Finnigan LCQ Advantage ion trap mass spectrometer (Thermo Finnigan, San Jose, CA) was used to obtain data up to MS^6 to confirm fragmentation pathways.

A modified VG ZAB-3F tandem mass spectrometer with BEE geometry (VG Analytical, Manchester, UK) was used to obtain metastable ion (MI) spectra and kinetic energy release data. In MS^3 experiments, the MH^+ ions (generated by self-chemical ionization) were selected by the magnet and subjected to collisional activation in the second field-free region (FFR); the resulting ions were then transmitted to the third FFR to record the MI spectra. Kinetic energy release values were calculated by established procedures[33] using the MI peak widths at half-height, which were measured at an energy resolution sufficient to reduce the width of the precursor ion main beam to ~5 V at half-height. The accelerating voltage was 8 kV; helium was used as the collision gas for the CID experiments at a cell pressure that causes 20% attenuation of the main beam.

Benzydamine (see below for the structure) and *N*,*N*,*N*′,*N*′-tetramethyl-1,3-propanediamine were purchased from Sigma or Aldrich Chemicals (St. Louis, MO), respectively, and used without further purification. For self-chemical ionization on the ZAB, the propanediamine was injected directly into the septum reservoir inlet. For electrspray experiments on other instruments, the compounds were dissolved in methanol containing 0.1% formic acid at a concentration of 1 μg/mL and infused with a syringe pump at a flow rate of 2 μL/min.

(33) Holmes, J. L.; Terlouw, J. K. *Org. Mass Spectrom*. **1980**, *15*, 383−396.

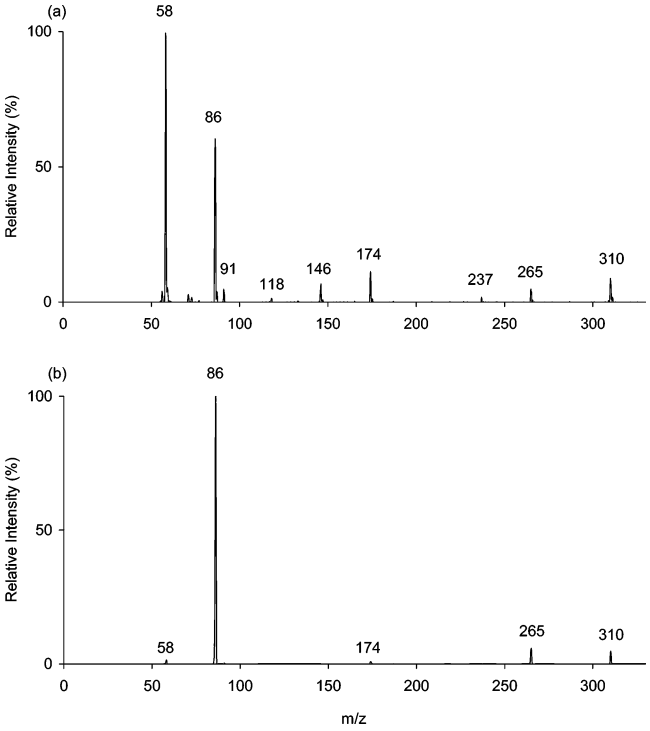

FIGURE 1. (a) Q1-scan mass spectrum of benzydamine at a DP voltage of 40 V and (b) CID mass spectrum of the MH^+ ion (*m/z* 310) of benzydamine at a collision energy of 25 eV (lab scale, N_2). Fragmentation efficiency is 95% in both cases.

Results and Discussion

When comparing the mass spectrum of a compound obtained by scanning Q1 (the first analyzer of a triple quadrupole) with the mass-selected CID spectrum of its molecular ion (MH^+), it is important to ensure that the energies imparted on the decomposing ions are similar at the two reaction venues. Since energy deposition in the orifice-skimmer region[15] is more complicated than in the collision cell, as stated earlier, we decide to use fragmentation efficiency (E_f) as an energy indicator, which is defined as[34]

$$E_f = \frac{\sum F_i}{\sum F_i + P}$$

where ΣF_i is the total intensity of all fragment ions, and P is the intensity of the remaining precursor (molecular) ion.

Representative mass spectra of benzydamine, one of each type, are shown in Figure 1. They were acquired at a declustering potential (DP) voltage of 40 V and a collision energy (lab scale) of 25 eV, respectively. A similar E_f is achieved in both cases; however, a striking difference is observed for the ion of *m/z* 58, which is the base peak in the Q1-scan spectrum but only 1% of the base peak in the CID spectrum. Fragmentation of the MH^+ ion of benzydamine proceeds in two series of reactions. As shown in Scheme 1, the initial simple bond cleavages take place on the side chain upon protonation

(34) (a) Yost, R. A.; Fetterolf, D. D. *Mass Spectrom. Rev.* **1983**, *2*, 1−45. (b) Ospina, M. P.; Powell, D. H.; Yost, R. A. *J. Am. Soc. Mass Spectrom*. **2003**, *14*, 102−109.

SCHEME 1

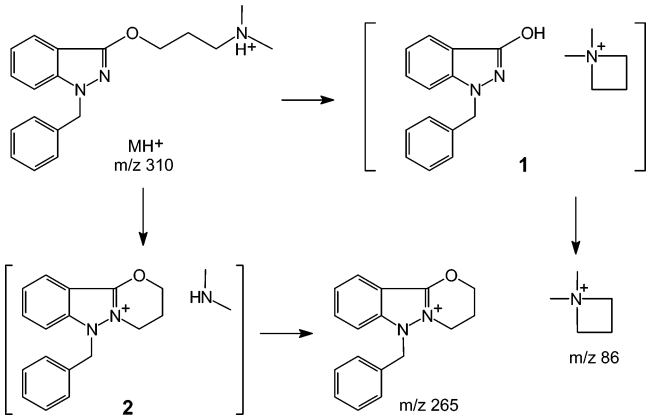

at the two heteroatoms. Loss of the terminal dimethylamine gives rise to the *m/z* 265 ion, from which further fragmentation product ions (*m/z* 174, 146, and 118) are formed in a stepwise manner as will be discussed later. In parallel, loss of the indazole ring leads to formation of the dimethylazetidine cation (*m/z* 86), which could expel an ethylene to form the *m/z* 58 ion.

A glimpse at the two spectra in Figure 1 could lead to a conjecture that the prominent *m/z* 58 ion comes from an impurity, because the Q1-scan produces a "full" spectrum of the sample, especially when the *m/z* 58 ion is not observed in the CID spectra at lower collision energies. We believe that the remarkable difference in intensity of the *m/z* 58 ion indicates that either this ion is formed by different mechanisms at different sites of observation or it is formed by the same mechanism that is, however, strongly favored in the orifice-skimmer region. When viewed from the side chain, benzydamine can be simplified as an α,ω-aminoether. In a series of high level theoretical calculations combined with experimental studies, Bouchoux and co-workers[35−37] have carefully characterized in details the unimolecular chemistry of α,ω-diols, diamines, and amino alcohols upon protonation. It has been shown consistently that when the HX-$(CH_2)_n$-XH_2^+ (n = 2−5; X = O, NH) ions eliminate the neutral XH_2 molecule, an ion-neutral complex of the protonated cyclic ether (or amine) with XH_2 is *always* formed as an intermediate, which lies in an energy well prior to the final products on the potential energy profiles.[35−37] For example, loss of ammonia from the MH^+ ion of 1,3-propanediamine proceeds via the [protonated azetidine/ammonia] complex.[36] In light of these findings, we believe that when benzydamine is protonated at the oxygen (initially or, more likely, by H-transfer from the nitrogen-protonated species), a similar ion-neutral complex, **1**, is also formed as shown in Scheme 1 on the pathway to the *N*,*N*-dimethylazetidine cation (*m/z* 86).

In the unimolecular chemistry of HX-$(CH_2)_n$-XH_2^+ (n = 2−5, X = O, NH), loss of water or ammonia is the predominant reaction. For those with n = 3, the elimination reaction leading to loss of [XH_2 + C_2H_4] from the

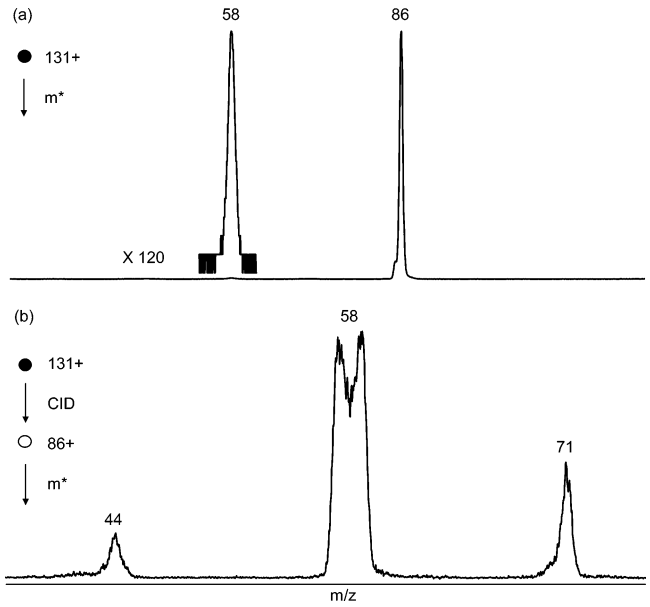

FIGURE 2. (a) MI mass spectrum of the MH^+ ion (*m/z* 131) of *N*,*N*,*N*′,*N*′-tetramethyl-1,3-propanediamine and (b) MI mass spectrum of the *m/z* 86 ion generated from CID in the second field-free region of the MH^+ ion of the diamine. Note that the *m/z* 58 peak in the top panel gives only a trivial kinetic energy release ($T_{0.5}$ = 0.8 kcal/mol), whereas the dish-topped peak at *m/z* 58 in the bottom panel shows a $T_{0.5}$ = 27 kcal/mol.

MH^+ ion is probably a minor reaction and was not discussed previously.[35−37] For 1,3-propanediamine, for example, the MH^+ ion could lose [NH_3 + C_2H_4] to generate the immonium ion, $CH_2{=}NH_2^+$. This reaction can take place in a stepwise manner (*m/z* 30 is a major ion in the CID spectra of the $[MH\text{-}NH_3]^+$ ion),[36] but is there any other mechanism by which this reaction may occur? New mechanistic information about this reaction should shed light on how to understand the difference observed in the mass spectra of benzydamine.

N,*N*,*N*′,*N*′-Tetramethyl-1,3-propanediamine (TMP) was chosen for further studies as a model molecule. In ESI-MS it gives only two fragment ions at *m/z* 58 and 86 in addition to its MH^+ ion at *m/z* 131. The intensity ratios of $58^+/86^+$ are consistently higher in Q1-scan spectra than in the CID spectra of its MH^+ ion when compared at the same fragmentation efficiencies, which is similar to that seen for benzydamine. On the ZAB mass spectrometer (BEE geometry), the metastable ion spectrum of its MH^+ ion, presented in Figure 2a, shows predominant loss of dimethylamine (*m/z* 86) and a very small, but not negligible, peak at *m/z* 58, which gives only a trivial kinetic energy release ($T_{0.5}$ < 1 kcal/mol). However, when the MH^+ ion (*m/z* 131) was subjected to collisional activation in the second FFR, the *m/z* 86 ion generated therein produced an MI spectrum (in the third FFR) that has a dish-topped peak at *m/z* 58 (Figure 2b) from which a $T_{0.5}$ = 27 kcal/mol is obtained.

The peak shapes and the kinetic energy release values for the *m/z* 58 ion from TMP indicate that this ion can be formed in two different ways. As shown in Scheme 2, the elimination of dimethylamine from the MH^+ ion is expected to go through transition state TS1 leading to the [dimethylazetidine cation/dimethylamine] complex, **3**, as a result of the intramolecular nucleophilic substitu-

(35) Bouchoux, G.; Choret, N.; Flammang, R. *J. Phys. Chem. A* **1997**, *101*, 4271−4282.
(36) Bouchoux, G.; Choret, N.; Berruyer-Penaud, F.; Flammang, R. *J. Phys. Chem. A* **2001**, *105*, 9166−9177.
(37) Bouchoux, G.; Choret, N.; Berruyer-Penaud, F.; Flammang, R. *Int. J. Mass Spectrom.* **2002**, *217*, 195−230.

SCHEME 2

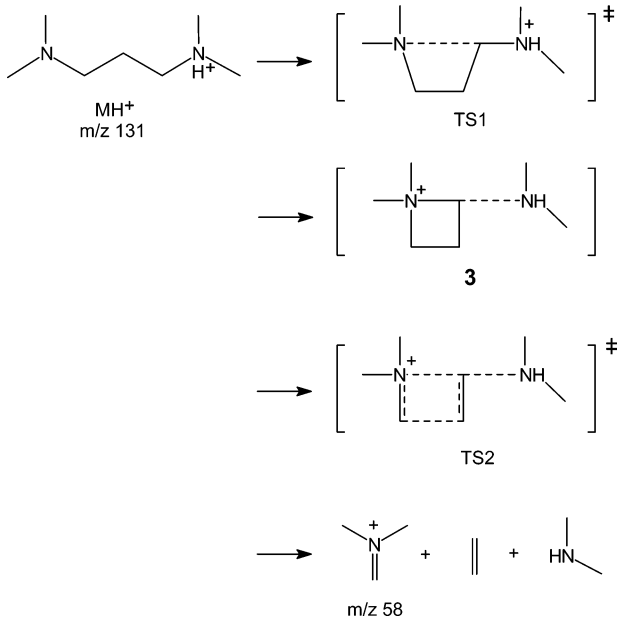

tion.[36] This ion-neutral complex is a watershed intermediate for two reaction channels. One is the simple separation of the two partners of the complex to give the *N*,*N*-dimethylazetidine cation (route not shown in Scheme 2). The cyclic structure of the cation, which is consistent with the unsubstituted azetidine analogue identified in similar fragmentation reactions by comparison with the authentic molecule,[36,37] is confirmed by our neutralization-reionization experiments.[38,39] To further lose an ethylene in a stepwise manner, the *isolated* azetidine cation has to open the ring to form a linear primary carbocation, $[(CH_3)_2N\text{-}(CH_2)_3^+]$, in the transition state (TS-C$^+$). This creates a high energy barrier and, therefore, a substantial reverse activation energy which is the main source of kinetic energy release. Alternatively, another channel via transition state TS2 could lead to loss of dimethylamine *and* ethylene. Within the ion-neutral complex, **3**, the neutral dimethylamine may play a significant role in stabilizing the structure that is evolving toward the elimination of ethylene from azetidine to form the immonium ion (*m/z* 58). Elongation of the N^+-CH_2 bond results in partial transfer of the formal charge on the quaternary nitrogen to the C atom, which is then stabilized by the neutral amine that is still associated with the ionic partner. This transition state, TS2, is much lower in energy than the ring-opened structure (TS-C$^+$).

By using the thermochemical data[40−42] given in Table 1, a potential energy profile is created as illustrated in Figure 3a for the reactions of TMP, including loss of ethylene directly from the [dimethylazetidine cation/dimethylamine] complex. The transition states, TS1 and TS2, are placed slightly higher than the thresholds for the two reaction channels (TS1 is the only barrier for the *m/z* 86 ion), in view of the minor kinetic energy releases. They are also approximately 15 kcal/mol apart. This energy difference is in keeping with the metastable ion time window, to allow observation of both the *m/z* 86 *and* *m/z* 58 ions that are considerably different in intensity (Figure 2a). For the fragmentation reaction of the dimethylazetidine cation alone, the potential energy profile is overlaid in Figure 3b, whereby the reverse activation energy of the reaction is estimated to be 43 kcal/mol, in

TABLE 1. Heats of Formation of Related Species (kcal/mol)

species	ΔH_f°	ref/note
C_2H_4	12.5	40
$(CH_3)_2NH$	−4.7	40
$(CH_3)_2N^+{=}CH_2$	158	40
$(CH_3)_2N{-}(CH_2)_2CH_2^+$	214	41
[azetidine + H]$^+$	163.5	36, 40, 42[a]
[*N*,*N*-dimethylazetidine]$^+$	153	estimated[b]
[TMP + H]$^+$	110.6	40, 42[a]

[a] Calculated from the heat of formation and proton affinity of the molecule. [b] From protonated azetidine an increment of −5 kcal/mol is assumed for substitution of a methyl for hydrogen as seen in various R-NH_3^+, R-$NH_2^+(CH_3)$, and $RNH^+(CH_3)_2$ ions.

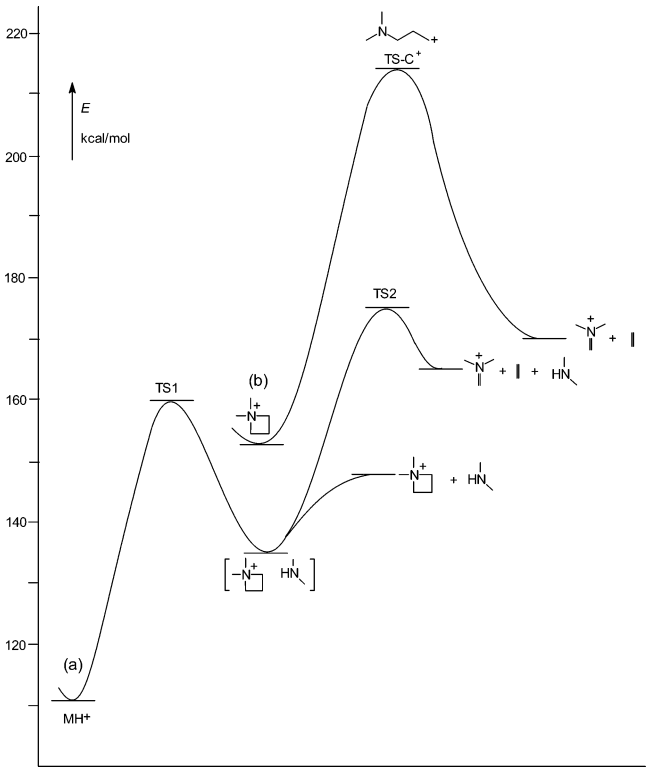

FIGURE 3. Potential energy profiles for (a) losses of dimethylamine and [dimethylamine + ethylene] by way of an azetidine/amine complex from the MH$^+$ ion of *N*,*N*,*N*′,*N*′-tetramethyl-1,3-propanediamine, and (b) elimination of ethylene from isolated *N*,*N*-dimethylazetidine through the ring-opened primary carbocation transition state.

(38) In the neutralization-reionization mass spectrum of the [TMP + H]$^+$ ion (see Supporting Information), the peak observed at *m/z* 71 corresponds to the M$^{+\bullet}$ ion of *N*-methylazetidine that was generated from the *N*,*N*-dimethylazetidine cation precursor. The quaternary ammonium cation loses one methyl upon neutralization (the quaternary ammonium radical is unstable).

(39) For a review on neutralization-reionization mass spectrometry, see: Holmes, J. L. *Mass Spectrom. Rev.* **1989**, *8*, 513−539.

(40) Lias, S. G.; Bartmess, J. E.; Liebman, J. F.; Holmes, J. L.; Levin, R. D.; Mallard, W. G. *J. Phys. Chem. Ref. Data* **1988**, *17* (Suppl. 1), 1−861.

(41) Bowen, R. D.; Colburn, A. W.; Derrick, P. J. *J. Chem. Soc., Perkin Trans. 2* **1993**, 2363−2372.

(42) Hunter, E. P. L.; Lias, S. G. *J. Phys. Chem. Ref. Data* **1998**, *27*, 413−656.

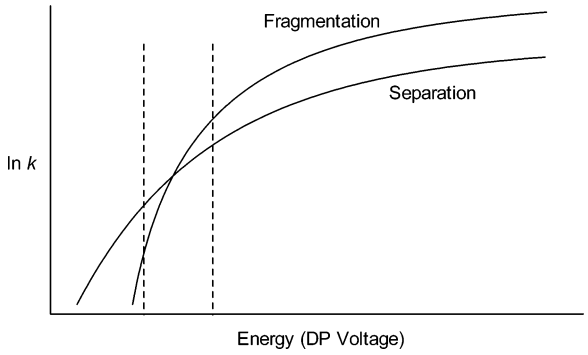

FIGURE 4. A schematic presentation of changes in rate constants with energy (declustering voltage) for simple separation and the secondary fragmentation of a solvated ion-neutral complex.

good agreement with the substantial kinetic energy release shown in Figure 2b. Since the ring-opened transition state (TS-C^+) is approximately 40 kcal/mol in energy above the transition state TS2 (note that the ΔH_f° of dimethylamine is very small, Table 1), preference should be given to the ion-neutral complex mediated mechanism (Scheme 2) for the generation of *m/z* 58 from the MH^+ ion.

In the case of benzydamine, the equivalent ion-neutral complex, species **1** in Scheme 1, should play the same role in the formation of both the *m/z* 86 and *m/z* 58 ions as in the TMP case described above. For the latter (*m/z* 58) a transition state similar to TS2 will also be evolved from the complex. However, although these two ions are both formed via the same ion-neutral complex, they are produced in different types of reactions. One is a simple separation with only a small amount of energy required and the other is a secondary fragmentation that may have a significant energy barrier. Solvation should have opposite effects on the activation energy of these two types of reactions and therefore should also alter their reaction rate vs energy relationships. As demonstrated in Figure 4, the two curves for simple separation and fragmentation cross at a certain energy point because of the different activation energies and frequency factors of the reactions. Solvation results in a tighter enclosure of the ion-neutral complex (cage effects), which obviously obstructs the separation of the two partners but enhances their interaction. Since this interaction is essential in stabilizing the transition state in the fragmentation (Scheme 2), solvation is expected to intensify the stabilization effect and thus reduces the activation energy. As a result of these opposite effects on the reactions, when the solvation effect is removed (such as in the mass-selected CID experiments), the crossing point of the two curves in an *unsolvated* system will shift up to a higher energy level, which could be beyond the window (the dotted lines) of achievable energies.

To characterize in depth the solvation effects on reactions mediated by ion-neutral complexes, benzydamine was further investigated under different conditions (and on different instruments with different ESI source structures, to be discussed below). Presented in Figure 5 are three breakdown graphs of benzydamine obtained either by scanning Q1 or Q3 directly or by mass-selected CID over similar energy ranges. In CID reactions (Figure 5c) *m/z* 86 is the predominant product ion with only minor *m/z* 58 over the entire energy range studied. However, in Q1 scan at DP = 40 V, for example, *m/z* 58 dominates the spectrum (Figures 1a and 5a) and continues to mount as the DP voltage increases. An interesting contrast between the two breakdown graphs (Figure 5a and c) is that in CID the intensity ratios of $58^+/86^+$ remain constantly low even when the E_f has *already* reached 100%, whereas in Q1 scans the same ratio climbs rapidly even though the E_f reaches *only* up to 96% at higher DP voltages. It seems that the crossing point of the *m/z* 86 and 58 curves in Figure 5a corresponds to the crossing point of the ln *k* vs *E* curves in Figure 4. Thus, the experimental results for the reactions in the orifice-skimmer region can be well interpreted by the reaction rate hypothesis proposed for a *solvated* ion-neutral complex. In the CID experiments, where the decomposing ions are mass-selected and therefore solvation effects do not exist, the crossing point in Figure 4 has apparently moved up to above the energy window, and as a result, the simple separation prevails.

The breakdown graph of benzydamine for Q3 scans (Figure 5b) is also instructive. In Q3 scans, the first two quadrupoles are both set in the radio-frequency-only mode so that *all* ions (including solvated ones) generated in the ion source can pass through them and are analyzed by the third quadrupole. Small voltage gradients are applied to all lenses across Q1 and Q2 (the collision cell) to keep the ions moving, and Q2 is filled with nitrogen gas (for focusing purposes). Obviously, in this mode the solvated ions are allowed to travel a longer path and a longer time beyond the orifice-skimmer region (compared to that in Q1 scans). As a result of the extended oscillation, the desolvation efficiency will be improved and the population of desolvated ions will increase in the whole expanded reaction region (from the orifice downstream to the collision cell prior to the analyzing Q3). What is reflected in the Q3-scan spectra is the increased contribution of fragmentation from *desolvated* ions. Therefore, the relative intensity of *m/z* 86 is slightly higher in Figure 5b than in Figure 5a, but *m/z* 58 is the opposite (slightly lower in Figure 5b) at all same DP voltages, both due to the improved overall desolvation. As a result, the *m/z* 86 and 58 curves in Q3 scans cross at a DP voltage that is approximately 30 V higher than in Q1 scans. If the desolvation could further improve, the energy at which the two curves cross would be even higher. In keeping with this trend, therefore, in the *unsolvated* system (in the mass-selected CID), the two curves for *m/z* 86 and 58 in Figure 5c do not yet cross in the energy range studied.

For all three types of experiments, a comparison of energies required to achieve the same fragmentation efficiencies reveals additional information. The DP voltage in Q1 and Q3 scans can be linearly correlated with the collision energy in CID (see Supporting Information), which is similar to that reported by others,[16,17] indicating that the decomposing ions can be activated to the same energy levels by adjusting appropriate voltages at different observation sites. It is also noted that to achieve the same E_f, the DP voltage needed in Q3-scan is always *lower* than in Q1-scan by approximately 5 V. This is consistent with the fact that the path for transmission of ions in Q3-scan is increased and additional collisions to further activate the ions occur. However, in the three

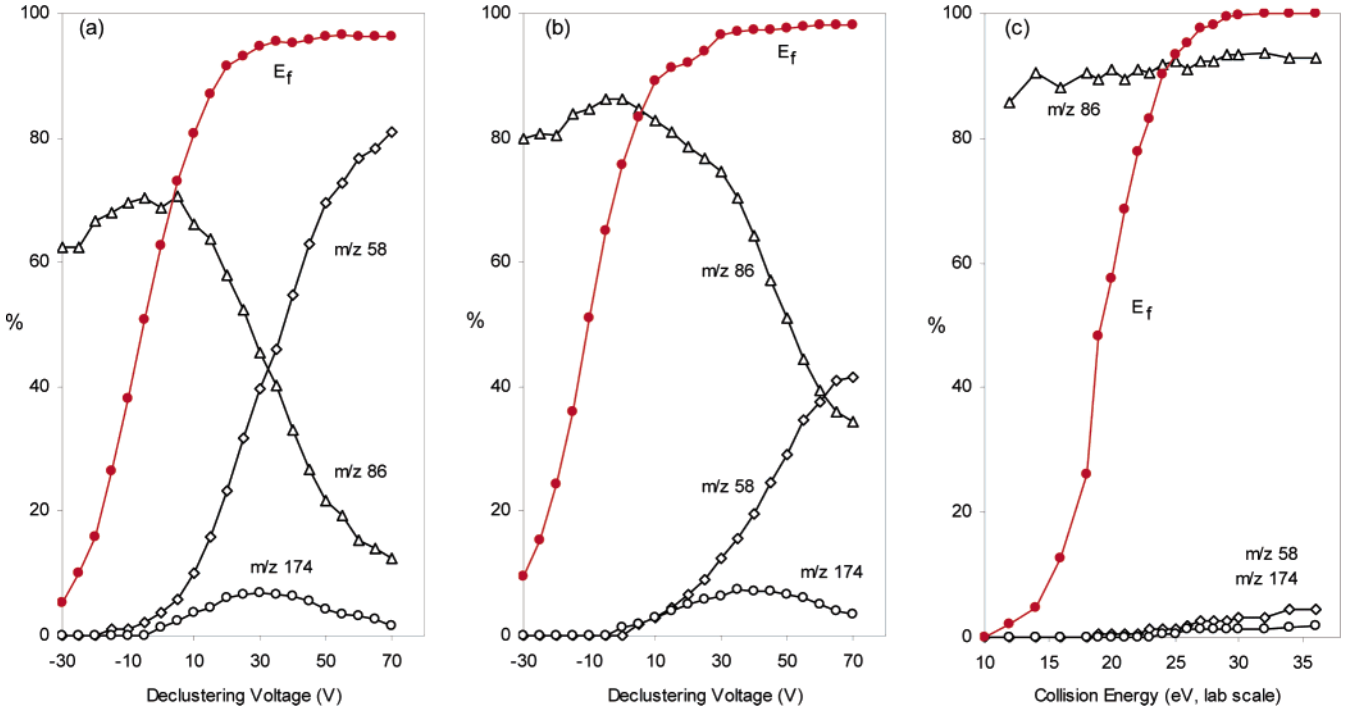

FIGURE 5. Breakdown graphs of benzydamine by (a) scanning Q1, (b) scanning Q3, and (c) mass-selected CID of the MH^+ ion, expressed as % of total fragmentation, with identical ion source conditions in all three types of experiments. Other minor ions are not shown. Curves are overlaid with that for the fragmentation efficiency (in red).

types of experiments, changes in the intensity of the *m/z* 58 ion over the energy windows are strikingly different. This ion is formed in a secondary fragmentation of an ion-neutral complex (Schemes 1 and 2). In different experiments, the extent to which the ion-neutral complex is solvated varies. Highly solvated species are subjected to Q1 analysis immediately; solvation is reduced in the extended drifting prior to Q3 analysis, and no solvation is present in the mass-selected CID. A comparison of the *m/z* 58 curves shown in the three panels of Figure 5 makes it salient that solvation has a strong effect on the reaction kinetics, in *favor* of the secondary fragmentation that occurs within the ion-neutral complexes.

It is also noteworthy that on different instruments the reactions of benzydamine *varied* in the ESI source but remained *identical* in mass-selected CID. As shown in Figure 1a, the immonium ion (*m/z* 58) accounted for 55% of the total fragmentation that occurred in the source region on the Sciex API 300. This ion was 28% and 12%, respectively, observed on the Sciex API 4000 and the Micromass Ultima in the same region at the same fragmentation efficiency ($E_f = 95\%$). In contrast, this ion remained low in intensity (only 1−3%) in all CID spectra at the same E_f. These three instruments were operated with ion sources that have different desolvation powers. The results indicate again that the kinetics for the reaction leading to the immonium ion is indeed affected substantially by the desolvation efficiency.

In the mass spectra of benzydamine, in addition to the *m/z* 86 and 58 pair, another pair of ions at *m/z* 265 and 174 was also observed (Figure 1). Loss of the terminal dimethylamine from the MH^+ ion, which gives rise to the *m/z* 265 ion, is similar to the elimination of ammonia from the MH^+ ion of 1,3-aminopropanol.[37] While a similar oxetane/ammonia complex[37] is plausible, an alternative intermediate, species **2** in Scheme 1, would be preferred because a less strained six-membered ring is formed by offering the adjacent nitrogen in the reaction. The *m/z* 174 ion is the product ion from *m/z* 265 in subsequent loss of the benzyl group. It is interesting that the *m/z* 174 ion showed slightly but obviously higher intensities in Q1 and Q3 scans than in the CID spectra (Figures 1 and 5). This implies that solvation probably also affects the reaction by which this ion is formed from the ion-neutral complex (**2**). To discuss the solvation effects on this reaction, additional experiments were performed to elucidate the reaction mechanisms by which the *m/z* 174 ion is generated and further dissociated.

In the CID mass spectra of the *m/z* 265 ion, two major product ions that are complementary were observed at *m/z* 174 and 91, indicating cleavage of the benzyl−N bond with possibly a charge transfer between the two fragments. It was found that the intensity ratio of $91^+/174^+$ increased with increasing collision energy. This led us to propose a mechanism shown in Scheme 3. The heterolytic fission of the benzyl−N bond produces the benzyl cation and the neutral indazolone, which are associated as an ion-neutral complex. From this intermediate, the simple separation competes with the charge-transfer reaction. At a higher collision energy, which corresponds to a higher kinetic energy of the decomposing ion, the lifetime of the ion-neutral complex will be shorter, giving less time for further reactions between the two partners. Therefore, the charge-transfer reaction leading to *m/z* 174 is unfavorable at higher collision energies.

The charge-transfer reaction proposed in Scheme 3 is interesting and possible. The neutral indazolone would be similar to a tertiary aniline in terms of ionization energy (IE). The IE value of the benzyl radical[40,43] is 7.24

SCHEME 3

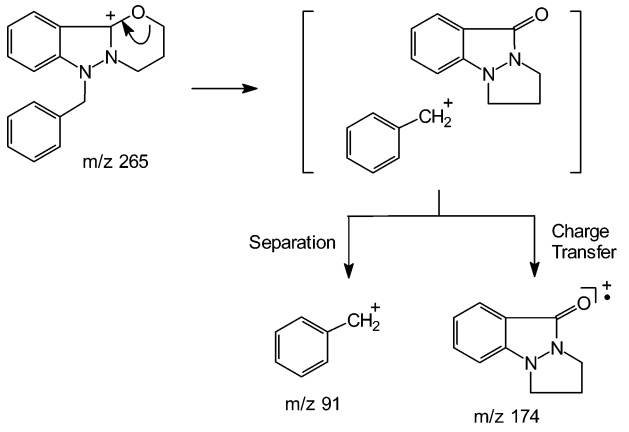

eV, and that of tertiary anilines[40,44] ranges from 6.9 to 7.4 eV. With such low ionization energies, both species are similarly vulnerable to loss of an electron. The reaction also involves flipping of the propylene along the indazolone ring. Further fragmentation of the *m/z* 174 ion should reveal structural information to support the reaction mechanism proposed. Therefore the *m/z* 174 ion was selected and subjected to collisional activation. It is interesting that its CID spectrum shows fragment ions at *m/z* 146, 118 and 90, in three consecutive losses of 28 mass units. This would be a repeat of the old story about high resolution in a different way. The Q-TOF mass spectrum shows that the *m/z* 174 ion loses 28.0314, 28.0064, and 27.9940 successively, corresponding to C_2H_4, N_2, and CO, respectively. On the ion trap mass spectrometer performing MS^6 experiments, the following gas-phase fragmentation sequence was determined: 310^+-$(MH^+) \rightarrow 265^+ \rightarrow 174^+ \rightarrow 146^+ \rightarrow 118^+ \rightarrow 90^+$. On the basis of the structure proposed for *m/z* 174 in Scheme 3, the above sequential fragmentation could be rationalized (see the Supporting Information).

With the background chemistry of the *m/z* 174 ion presented, it is easier to discuss the solvation effects on the reaction by which this ion is formed. In the intermediate complex **2** (Scheme 1), the neutral dimethylamine plays a critical role when the ionic partner evolves toward the structure of the *m/z* 174 ion shown in Scheme 3. Isomerization of the ionic species begins with the elongation of the $O-CH_2$ bond, in which the formal charge is partially transferred to the C atom. This, however, can be stabilized by the neutral dimethylamine. More importantly, solvation of the ion-neutral complex (**2**) *enhances* the interaction between the neutral and the ionic partners and thus increases the stabilization effects. Therefore, when the reaction is observed in the ion source (by Q1 or Q3 scans), the strong solvation in this region results in increased production of the *m/z* 174 ion, the complementary ion of *m/z* 91 and even the continued fragmentation of *m/z* 174 (to give *m/z* 146 and 118), which are either absent or only barely seen in the CID spectrum (Figures 1 and 5). The solvation effect on this reaction is similar to that observed in the reaction involving the *m/z* 86 and 58 ions discussed earlier.

In ESI-MS, the solvent plays an important role in the ionization of various molecules. More recently, it has been shown that solvents are also involved in the in situ reactions in the ESI source for the preparation of the ions of interest (e.g., complexes of transition metal ions). Different solvents used in the preparation could lead to ions of different structures,[45−47] and more interestingly, isomerization of the ions can be assisted by the solvent.[48] In the present study, we have demonstrated another aspect of the solvent effects on fragmentation reactions in mass spectrometry. Solvation of the ion-neutral complex intermediates could result in changes in activation energies and kinetics of the fragmentation reactions.

Conclusions

It was found that the Q1-scan spectra of benzydamine in ESI are dramatically different from the mass-selected CID spectra of its MH^+ ion. The *N*,*N*-dimethylimmonium ion, which dominates in Q1 scans at higher energies, is a minor product ion in the CID spectra. The fragmentation takes place by way of an intermediate ion-neutral complex composed of the *N*,*N*-dimethylazetidine cation and a neutral species. This reaction intermediate evolves to a transition state, which is stabilized by the neutral species of the complex, in the secondary fragmentation toward formation of the immonium ion. Solvation of the ion-neutral complex exerts opposite effects on the reaction kinetics of the simple separation and the secondary fragmentation of the complex. This is clearly demonstrated by applying three different experimental methods, whereby the decomposing ions are solvated to different degrees, and by using three different instruments with ion sources that are designed to have different desolvation efficiencies.

Acknowledgment. Y.-P.T. thanks Dr. John L. Holmes, University of Ottawa, for offering access to the VG ZAB-3F mass spectrometer for the MI and NRMS experiments and many discussions during a visit to his laboratory, and Dr. Alex. G. Harrison, University of Toronto, and Dr. Guy Bouchoux, Ecole Polytechnique, France, for their interest and valuable comments.

Supporting Information Available: Neutralization-reionization mass spectrum of the $[TMP + H]^+$ ion, a graph showing correlation of DP voltages with collision energies, and a proposed fragmentation mechanism for the *m/z* 174 ion. This material is available free of charge via the Internet at http://pubs.acs.org.

JO050398N

(43) Eiden, G. C.; Weisshaar, J. C. *J. Phys. Chem.* **1991**, *95*, 6194−6197.
(44) Farrell, P. G.; Newton, J. *J. Phys. Chem.* **1965**, *69*, 3506−3509.
(45) (a) Rogalewicz, F.; Hoppilliard, Y.; Ohanessian, G. *Int. J. Mass Spectrom.* **2000**, *201*, 307−320. (b) Hoppilliard, Y.; Rogalewicz, F.; Ohanessian, G. *Int. J. Mass Spectrom.* **2001**, *204*, 267−280. (c) Rogalewicz, F.; Hoppilliard, Y.; Ohanessian, G. *Int. J. Mass Spectrom.* **2001**, *206*, 45−52. (d) Rogalewicz, F.; Hoppilliard, Y.; Ohanessian, G. *Int. J. Mass Spectrom.* **2003**, *227*, 439−451.
(46) Desaire, H.; Leavell, M. D.; Leary, J. A. *J. Org. Chem.* **2002**, *67*, 3693−3699.
(47) Adhiya, A.; Wesdemiotis, C. *Int. J. Mass Spectrom.* **2002**, *214*, 75−88.
(48) Rodriguez-Santiago, L.; Noguera, M.; Sodupe, M.; Salpin, J. Y.; Tortajada, J. *J. Phys. Chem.* **2003**, *107*, 9865−9874.